0026-895X/06/7003-860–868$20.00
MOLECULAR PHARMACOLOGY
Copyright © 2006 The American Society for Pharmacology and Experimental Therapeutics
Mol Pharmacol 70:860–868, 2006

Vol. 70, No. 3
21923/3133851
Printed in U.S.A.

Phospholipase C-β3 and -β1 Form Homodimers, but Not Heterodimers, through Catalytic and Carboxyl-Terminal Domains

Yong Zhang, Walter K. Vogel, Jennifer S. McCullar, Jeffrey A. Greenwood, and Theresa M. Filtz

Department of Pharmaceutical Sciences, College of Pharmacy (W.K.V., T.M.F.), Department of Biochemistry and Biophysics (J.A.G., T.M.F.), and the Molecular and Cellular Biology Program (Y.Z., J.S.M., T.M.F.), Oregon State University, Corvallis, Oregon

Received December 28, 2005; accepted June 8, 2006

ABSTRACT

Phospholipase C-β (PLC-β) isoenzymes are key effectors in G protein-coupled signaling pathways. Prior research suggests that some isoforms of PLC-β may exist and function as dimers. Using coimmunoprecipitation assays of differentially tagged PLC-β constructs and size-exclusion chromatography of native PLC-β, we observed homodimerization of PLC-β3 and PLC-β1 isoenzymes but failed to detect heterodimerization of these isoenzymes. Size-exclusion chromatography data suggest that PLC-β3 and PLC-β1 form higher affinity homodimers than PLC-β2. Evidence supportive of limited PLC-β monomer–homodimer equilibrium appears at ≤100 nM. Further assessment of homodimerization status by coimmunoprecipitation assays with differentially tagged PLC-β3 fragments demonstrated that at least two subdomains of PLC-β3 are involved in dimer formation, one in the catalytic X and Y domains and the other in the G protein-regulated carboxyl-terminal domain. In addition, we provide evidence consistent with the existence of PLC-β homodimers in a whole-cell context, using fluorescent protein-tagged constructs and microscopic fluorescence resonance energy transfer assays.

Phospholipase C (PLC) is a key effector enzyme in multiple cellular signaling pathways, hydrolyzing phosphatidylinositol 4,5-bisphosphate to inositol 1,4,5-triphosphate and diacylglycerol, second messengers that subsequently regulate Ca^{2+} release from intracellular stores and protein kinase C activation. PLC isozymes are grouped into five families based on structure and regulatory mechanism: PLC-β, PLC-γ, PLC-δ, PLC-ε, and PLC-ζ. The PLC-β family exists as four known homologs in mammals, β1–β4, all of which are involved in G protein-coupled receptor-mediated signaling cascades (Rhee, 2001; Saunders et al., 2002). Of the four isoenzymes, PLC-β1 and PLC-β3 are widely distributed and are often found coexpressed in a variety of tissues, including brain, liver, uterus, parotid gland, lung, platelets, and heart (Hansen et al., 1995; Fukami, 2002).

PLC-β isoenzymes contain sequences with homology to several characterized protein structural motifs commonly found in membrane associated, Ca^{2+} and lipid binding proteins. These structural domains include pleckstrin homology (PH), EF hand, and C2 homology regions, as well as a PDZ-binding domain at the C terminus. Highly conserved among PLC family members are two domains required for catalytic activity, designated X and Y, that structurally form a triose phosphate isomerase barrel (TIM) to create the catalytic pocket in the crystal form of PLC-δ (Rhee, 2001).

Unique among PLC family members, PLC-β isoenzymes contain a carboxyl-terminal (C-tail) domain of approximately 400 amino acids that is involved in membrane association

This work was supported by the Pharmaceutical Research and Manufacturer's Association Foundation (to T.M.F.), the American Foundation for Pharmaceutical Education (J.S.M.), an Oregon Sports Lottery Scholarship (to Y.Z.), and the National Institutes of Health, National Institute of General Medical Sciences grant R01-GM61244 (to T.M.F.). This publication was made possible, in part, by the Confocal Microscopy Facility of the Environmental Health Sciences Center at Oregon State University, with funding from the National Institute of Environmental Health Sciences, National Institutes of Health grants P30-ES00210 and 1S10-RR107903-01.

Article, publication date, and citation information can be found at http://molpharm.aspetjournals.org.

doi:10.1124/mol.105.021923.

ABBREVIATIONS: PLC, phospholipase C; PH, pleckstrin homology; SEC, size-exclusion chromatography; FRET, fluorescence resonance energy transfer; DMEM, Dulbecco's modified Eagle's medium; GFP, green fluorescent protein; CFP, cyan fluorescent protein; PCR, polymerase chain reaction; YFP, yellow fluorescent protein; aa, amino acid(s); HEK, human embryonic kidney; His_6, hexahistidine; TCA, trichloroacetic acid ; DTT, dithiothreitol; PMSF, phenylmethylsulfonyl fluoride; TCA, trichloroacetic acid; PAGE, polyacrylamide gel electrophoresis; TCEP, tris(2-carboxyethyl) phosphine hydrochloride.

and regulation by $G\alpha_q$ subunits. Crystallization of the isolated C-tail domain of a turkey PLC-β revealed a structure of three α-helices forming a coiled coil that associates as an antiparallel homodimer along its long axis (Singer et al., 2002). Size-exclusion chromatography data suggested that purified, concentrated, full-length rat PLC-β1 and turkey PLC-β migrated consistent with protein dimerization (Singer et al., 2002). However, no crystallographic data on any full-length PLC-β isozyme are available.

PLC-β isoenzymes are both activated by $G\alpha_q$ subunits and have inhibitory GTPase-activating protein activity toward $G\alpha_q$ subunits. Studies of regulated and regulatory activities of some PLC-β isoenzymes support a hypothesis that dimerization is involved in the active state of the enzymes (Paterson et al., 1995; Paulssen et al., 1996). However, purified PLC-β2 is reported to fractionate by size-exclusion chromatography (SEC) consistent with a monomeric species (Guo et al., 2005), suggesting that different PLC-β isoenzymes have different homomeric affinities.

All previous studies of PLC-β assessed oligomerization status after purification and concentration. Using coimmunoprecipitation assays of differentially tagged full-length PLC-β3 and fragments thereof, we demonstrated that PLC-β3 exists as a dimer in dilute cell lysates in the presence of detergent. In addition, we observe that the catalytic domain of PLC-β3 dimerizes independent of the C-tail domain of PLC-β3, suggesting that at least two separate domains are involved in the formation of PLC-β3 dimers. We also demonstrate fluorescence resonance energy transfer (FRET) between fluorescently tagged PLC-β3 constructs in a whole cell microscopy assay consistent with PLC-β homodimerization in situ.

Materials and Methods

Materials. Minimum essential medium and Dulbecco's modified Eagle's medium (DMEM) were purchased from Mediatech (Herndon, VA) and fetal bovine serum was purchased from Hyclone (Logan, UT). Antibodies purchased from Santa Cruz Biotechnology (Santa Cruz, CA) included anti-hexahistidine antibody (H-15), PLC-β-selective polyclonal antibodies (PLC-β1, G-12; PLC-β3, H-84), anti-green fluorescent protein (GFP)/cyan fluorescent protein (CFP) polyclonal antibody, horseradish peroxidase-conjugated goat anti-rabbit secondary antibody, and horseradish peroxidase-conjugated goat anti-mouse secondary antibody. Anti-FLAG epitope (M5) monoclonal antibody was purchased from Sigma (St. Louis, MO), and anti-c-Myc epitope tag monoclonal antibody (Ab-1) was purchased from Oncogene (La Jolla, CA). SuperSignal West Pico chemiluminescent substrate was from Pierce (Rockford, IL). All restriction endonucleases were purchased from Promega (Madison, WI). High-Five insect (*Trichoplusia ni*) cells, Express Five SFM media, DNA polymerase Platinum *Pfx*, and pCDNA3.1(+) vector were obtained from Invitrogen (Carlsbad, CA). pCMV-Myc and pECFP-C1 vectors were from Clontech (Mountain View, CA). Protein A-Sepharose, size-exclusion chromatography molecular weight standards, and all chromatographic media were purchased from GE Healthcare (Little Chalfont, Buckinghamshire, UK), except CHT, which was from Bio-Rad Laboratories (Hercules, CA). Vectors containing human PLC-β3 and human PLC-β1a cDNA sequences were gifts from Dr. Günther Weber (Karolinska Institutet, Stockholm, Sweden) and Dr. Lucio Cocco (University of Bologna, Bologna, Italy) respectively. Baculovirus expression vectors containing cDNA sequence for rat PLC-β1, human PLC-β2, and amino-terminally hexahistidine-tagged (His_6) human PLC-β3 were provided by Drs. T. Kendall Harden and John Sondek, respectively (School of Medicine, University of North Carolina at Chapel Hill, Chapel Hill, NC).

Plasmid Construction. Sequence for the FLAG tag epitope DYKDDDDK (Chubet and Brizzard, 1996) was inserted into the multiple cloning site of the mammalian expression vector pCDNA3.1(+) using two complementary oligonucleotides. The resultant vector, pDNA3.1(+)-FLAG, allows for in-frame addition of a FLAG epitope tag to the amino terminus of an inserted sequence. YFP fragment was amplified by PCR and inserted into pDNA3.1(+) for construction of the pDNA3.1(+)-YFP vector. The mammalian expression plasmids pDNA3.1(+)-FLAG, pCMV-Myc, pDNA3.1(+)-YFP, and pECFP-C2 will express Flag tag, Myc tag, YFP, or CFP, respectively, at the amino terminus of an in-frame inserted sequence.

Full-length PLC-β3 cDNA sequence was subcloned into pCMV-Myc, pDNA3.1(+)-YFP, and pCDNA3.1(+)-FLAG plasmids using EcoRI and XhoI restriction sites, creating the vectors pCMV-Myc-PLC-β3, pCDNA3.1(+)-YFP-PLC-β3, and pCDNA3.1(+)-FLAG-PLC-β3. Full-length PLC-β3 cDNA sequence was subcloned into pECFP-C2 using EcoRI and HindIII restriction sites, creating the vector pECFP-C2-PLC-β3, which expresses CFP fused to the amino terminus of full-length PLC-β3. A QuikChange site-directed mutagenesis kit (Stratagene, La Jolla, CA) was used to delete base pairs 'TG' of the stop codon sequence for PLC-β3 and provide the correct reading frame for fusion with the yellow fluorescent protein (YFP) sequence in the pEYFP-N2 plasmid. The vector pPLC-β3-N2-EYFP expresses YFP fused to the carboxyl terminus of full-length PLC-β3.

Fragments of PLC-β3 were amplified by PCR to incorporate 5′ EcoRI and 3′ XhoI restriction sites using the following sets of primers: amino-terminal PH and EF hand domains (NT-β3; aa 2–315) amplified with 5′-ATATATGAATTCTGGCGGGCGCCCAG-3′ and 5′-ATATTCTCGAGTCACAGATCCAGGGCTTC-3′; catalytic X and Y domains and intervening sequence (XY-β3; aa 310–730) amplified with 5′-ATATATGAATTCTGCTGGAAGCCCTGGAT-3′ and 5′-TATATTCTCGAGTCAGACCCGCAAGGCATT-3′; C-tail domain (CT-β3, aa 861-1234) amplified with 5′-ATCGAATTCGGAACCCCATTAAGCACGTCAG-3′ and 5′-TTCTCGAGTCAGAGCTGCGTGTTCTCC-3′; and C2/C-tail-deleted mutants (ΔC-β3; aa 2–730) amplified with 5′-TATATGAATTCTGGCGGGCGCCCAG-3′ and 5′-TATATTCTCGAGTCAGACCCGCAAGGCATT-3′. PCR-amplified cDNA sequences for NT-β3 and ΔC-β3 were ligated into EcoRI and XhoI restriction sites in pDNA3.1(+)-FLAG and pCMV-Myc plasmids. XY-β3 and CT-β3 sequences were ligated into EcoRI and XhoI restriction sites in pCMV-Myc and pECFP-C2 plasmids. Protein structural domain boundaries for the protein fragments were defined by sequence alignment and analysis using ClustalW version 1.82.

Full-length human PLC-β1a cDNA sequence was amplified by PCR to incorporate 5′ SalI and 3′ KpnI restriction sites and then subcloned into pCMV-Myc and pECFP-C2, creating the plasmids pCMV-Myc-PLC-β1 and pECFP-C2-PLC-β1. All constructs were confirmed by sequencing.

Cell Culture and Transfection. Human embryonic kidney (HEK) 293 cells were cultured in 90% minimum essential medium, 10% fetal bovine serum, 100 units/ml penicillin, and 0.1 mg/ml streptomycin at 37°C under 5% CO_2 in humidified air. The day before transfection, HEK 293 cells were plated at a density of 8×10^5 cells/10-cm dish. QIAGEN (Valencia, CA) midiprep-purified DNA plasmids (5 μg total) were transiently transfected into HEK 293 cells by a calcium phosphate precipitation method as described previously (Avram et al., 1999). Human astrocytoma 1321N1 cells were cultured in 90% DMEM, 10% fetal bovine serum, 100 units/ml penicillin, and 0.1 mg/ml streptomycin at 37°C under 5% CO_2 in humidified air as described previously (Filtz et al., 1994). Native PLC-β1, PLC-β2, and hexahistidine-tagged PLC-β3 were expressed in High-Five cells in suspension culture after baculovirus infection at a multiplicity of infection of 1 to 3. The cells were grown in Express Five SFM media at 27°C and harvested 48 h after infection as described previously (Paterson et al., 1995; Snyder et al., 2003).

Whole-Cell Inositol Phospholipid Hydrolysis Assays. HEK 293 cells were assayed for basal inositol phosphate accumulation essentially as described previously (Filtz and Niibori, 2004) with the following modifications. HEK 293 cells were seeded into 24 well plates at a density of 3×10^4 cells/well and allowed to attach overnight. Cells were transfected as described above with 0.2 μg of plasmid DNA/well. Forty-eight hours after transfection, HEK 293 cells were labeled for 18 h overnight with 1 μCi/well [^{3}H]inositol in inositol-free DMEM. Medium was changed to 10 mM HEPES-buffered DMEM, pH 7.4, and cells were moved to a 37°C waterbath in room air. LiCl (10 mM; inositol phosphatase inhibitor) was added to all wells at time 0 and the assays stopped after 30 min by addition of 5% trichloroacetic acid (TCA). ^{3}H-inositol phosphates accumulated in the presence of LiCl were collected by anion exchange chromatography and quantitated as described previously (Filtz and Niibori, 2004).

Coimmunoprecipitation. HEK 293 cells were washed thrice with ice-cold phosphate-buffered saline 48 h after transfection, collected by scraping, and pelleted at 500*g* for 5 min. Ice-cold lysis buffer (0.6 ml; 10 mM Tris, pH 7.4, 5 mM $MgCl_2$, 2 mM EDTA, 0.1 mM PMSF, 1 μM pepstatin A, and 10 μM leupeptin) was added to each sample and incubated on ice for 10 min. Cells were lysed with 15 strokes of a Dounce homogenizer, and the lysate was centrifuged at 500*g*, 4°C for 5 min to pellet nuclei and intact cells. Two different extraction protocols were used to prepare samples containing soluble PLC-β. For detergent extraction, the low speed supernatant was diluted in 1 volume of triton extraction buffer (100 mM HEPES, pH 7.4, 5 mM EDTA, 300 mM NaCl, 1% Triton X-100, 2 mM DTT, 0.1 mM PMSF, 1 μM pepstatin A, and 10 μM leupeptin) and incubated at 4°C for 1 h with inversion followed by centrifugation at 16,000*g* for 30 min at 4°C to pellet insolubles. For high pH extraction, 50 mM Na_2CO_3 was added to the low speed supernatant and incubated at 4°C for 1 h with inversion followed by centrifugation at 16,000*g* for 30 min at 4°C. The high pH extraction supernatant was neutralized to pH 7.3 with HCl.

Immunoprecipitation from cell extracts was accomplished as described previously (McCullar et al., 2003). All antibodies were used at a concentration of 0.1 μg/ml, except anti-FLAG M5 at 2 μg/ml and secondary anti-IgG antibodies at 0.04 μg/ml. Immunoreactive bands were visualized using SuperSignal West Pico chemiluminescent substrate followed by exposure to X-ray film for 20 to 30 s. X-ray film images of all immunoblots were quantitated by densitometry and analysis with NIH ImageJ software ver. 1.36b (http://rsb.info.nih.gov/nih-image/).

Trichloroacetic Acid Precipitation. Cell lysates, prepared as above, were precipitated with 15% TCA on ice for 10 min, followed by centrifugation at 16,000*g* for 15 min at 4°C. The acid precipitated pellets were washed with 500 μl of ice-cold acetone and recentrifuged at 16,000*g* for 15 min at 4°C; the pellets were dried before separation by SDS-PAGE.

Purification of PLC-β Subtypes from 1321N1 Cells. Cells were hypotonically lysed and Dounce-homogenized in 10 mM HEPES, pH 7.4, 1 mM EDTA, 2 mM $MgCl_2$, 1 mM DTT, and protease inhibitors (0.1 mM PMSF, 1 μM pepstatin A, 10 μM leupeptin, 2 mM benzamidine, and 10 μg/ml E-64). Cell debris and nuclei were pelleted at 1000*g*. The postnuclear supernatant was extracted with 0.5% *n*-octyl-β-D-glucopyranoside. The clarified extract was adsorbed on to a Q-Sepharose FF column equilibrated with buffer A (25 mM HEPES, pH 7.4, 1 mM EDTA, 1 mM DTT, 0.1 mM PMSF) plus 100 mM NaCl. The column was eluted with buffer A plus 350 mM NaCl directly onto a heparin-Sepharose HP column. PLC-β3 was eluted by increasing NaCl to 700 mM. The heparin pool was buffer exchanged on G25-Sephadex equilibrated with 100 mM potassium phosphate, pH 7.2, 1 mM DTT, and 0.1 mM PMSF and adsorbed onto CHT. The CHT column was washed with 370 mM potassium phosphate, pH 7.2 and eluted with a 10-column volume gradient to 1 M potassium phosphate, pH 7.2. Peak fractions were analyzed by Western blot to identify PLC-β3 and confirm the lack of contamination with PLC-β1 subtype. To concentrate the sample, the CHT column pool was buffer exchanged on G25-Sephadex equilibrated with buffer A, adsorbed onto Q-Sepharose HP, and eluted with a six-column volume gradient from 100 to 350 mM NaCl in buffer A. PLC-β3 eluted as a shouldered peak centered at 260 mM NaCl.

Purification of Recombinant PLC-β from High-Five Cells. PLC-β1 and PLC-β2 isoenzymes were expressed in and purified from baculovirus-infected insect High-Five cells as described previously (Paterson et al., 1997). Amino-terminally hexahistidine-tagged recombinant PLC-β3 (His_6-PLC-β3) was purified from baculovirus-infected insect High-Five cell lysate. High-Five lysate was Dounce homogenized in 10 mM HEPES, pH 7.4, 0.5 mM EDTA, 1 mM TCEP, and protease inhibitors. Whole cell homogenate was layered on a 15%/45% sucrose step gradient in 25 mM HEPES, pH 7.4, 1 mM TCEP, and protease inhibitors, then centrifuged at 126,000*g* for 1.5 h. The 15% layer and the 15%/60% sucrose interface were collected and extracted by addition of NaCl to 500 mM and Na_2CO_3 to pH 10, followed by centrifugation at 504,000*g* for 1 h. The soluble extract was neutralized, imidazole was added to 20 mM, and extract was adsorbed to a Ni-Sepharose column. The column was washed with 20 mM HEPES, pH 7.4, 20 mM imidazole, 500 mM NaCl, 0.5 mM TCEP, 0.1 mM PMSF, 1 μM pepstatin A, and 2 mM benzamidine; His_6PLC-β3 was eluted in the same buffer with 250 mM imidazole. The amino-terminal hexahistidine tag was removed with tobacco etch virus protease (Kapust et al., 2001) at a ratio of 45:1 (PLCβ3/tobacco etch virus protease) during dialysis overnight against buffer A plus 100 mM NaCl. Subsequent chromatographic purification steps were as above for the purification from 1321N1 cells.

Size-Exclusion Chromatography. PLC-β proteins were analyzed on a Superdex 200 (1.0 × 30 cm) column equilibrated with 20 mM HEPES, pH 7.4, 140 mM NaCl, 0.5 mM EDTA, and 1 mM DTT and operated at 0.5 ml/min at 4°C. Protein elution from 100-μl injections was monitored by absorbance at 280 nm using a 0.5-cm in-line flow cell. For experiments at protein concentrations too low to be observed by absorbance, the eluate was fractionated. The fractions were precipitated in the presence of 50 μg of bovine serum albumin and 80% ice-cold acetone and detected by immunoblot analysis. Molecular mass was estimated from regression analysis (Siegel and Monty, 1966) of standard globular proteins. The protein standards (molecular mass and Stokes' radius as reported by the supplier) were thyroglobulin (669 kDa, 8.50 nm), ferritin (440 kDa, 6.10 nm), catalase (232 kDa, 5.22 nm), aldolase (158 kDa, 4.81 nm), bovine serum albumin (67 kDa, 3.55 nm), and ovalbumin (43 kDa, 3.05 nm).

Microscopic FRET Protocol. HEK 293 cells grown on glass coverslips were transiently transfected by the calcium phosphate precipitation method with 0.1 μg of plasmid DNA unless otherwise indicated. Cells were washed twice with PBS after 48 h transfection, fixed in 3% formaldehyde for 20 min, and mounted on slides with a ProLong antifade kit (Invitrogen).

Microscopic fluorescence intensity measurements for FRET analysis were obtained by the method of Karpova et al. (2003), which quantitates an increase in donor fluorescence after acceptor photobleaching. LP 530 and BP 470-500 filters were used for detection of YFP (acceptor) and CFP (donor) emission, respectively, on a Zeiss LSM510 confocal microscope (Carl Zeiss, Thornwood, NY) operating with a 30-mW argon laser tuned to 514 nm for YFP excitation and 458 nm for CFP excitation. Cells were examined with a 63× Zeiss oil immersion objective. For each cell, a region of interest was selected and photobleached at 514 nm (75% laser intensity) for 150 iterations. Before and after acceptor photobleaching, CFP and YFP images were collected to assess changes in donor and acceptor fluorescence. FRET efficiency in the region of interest was calculated as $E_F = (I_2 - I_1) \times 100/I_2$, where I_1 is the CFP intensity immediately before photobleaching and I_2 is the CFP intensity immediately after photobleaching. For every cell, a nonphotobleached region was monitored, and its FRET efficiency (E_C) over the same time frame was quantitated as a

background control. The average FRET efficiency is stated as ($E_F - E_C$) ± S.E.M. under *Results*.

For calculation of distance between fluorescent pairs in the dimer construct (r_0), we used the equation $E = R_0^6/(R_0^6 + r_0^6)$ where E is the average FRET efficiency as calculated above and R_0 is a Förster distance for CFP/YFP pairs of 4.9 nm as calculated previously (Patterson et al., 2000; Karpova et al., 2003).

Results

Identification of PLC-β3 Homodimers by Coimmunoprecipitation. To investigate PLC-β3 dimerization, a coimmunoprecipitation assay was performed with extracts of cells that had been transfected with vectors containing full-length PLC-β3 tagged at its amino terminus with either FLAG or Myc epitopes (FLAG-β3 or Myc-β3). HEK 293 cells were hypotonically lysed 48 h after transfection, extracted, and immunoprecipitated with anti-Myc-selective (Fig. 1, lanes 4, 7, and 8), anti-FLAG-selective (Fig. 1, lanes 3, 5, and 6), or anti-PLC-β3 carboxyl-terminal-selective (Fig. 1, lanes 2 and 9) antibodies. Immunoprecipitated samples were separated by SDS-PAGE, blotted onto nitrocellulose and probed with antibodies to detect anti-Myc, anti-FLAG, or anti-PLC-β3 immunoreactive species. The coexpression of Myc-β3 and FLAG-β3 in transfected HEK 293 cells after cotransfection of both Myc- and FLAG-tagged full-length PLC-β3-containing plasmids was confirmed by TCA precipitation of cell lysates (Fig. 1, lane 1) or immunoprecipitation of extracts with anti-PLC-β3-selective antibodies (Fig. 1, lane 2).

Neither FLAG, Myc, nor PLC-β3 immunoreactivity was detected in nontransfected HEK 293 cells (Fig. 1, lane 9). To demonstrate that epitope-tagged full-length PLC-β3 constructs were appropriately detected by selective anti-epitope tag antibodies but were not cross-reactive to other antibodies on immunoblot, HEK 293 cells were singly transfected with either pCDNA3.1(+)-FLAG-PLC-β3 or pCMV-Myc-PLC-β3. In cells transfected with a single construct, FLAG-β3 immunoprecipitated with anti-FLAG antibody was detectable on anti-FLAG or anti-PLC-β3 immunoblots, but not on anti-Myc immunoblots, at the expected molecular weight of approximately 150,000 (Fig. 1, lane 6). Conversely, Myc-β3 immunoprecipitated with anti-Myc antibody was detectable on anti-Myc or anti-PLC-β3 immunoblots, but not on anti-FLAG immunoblots, at the expected molecular weight (Fig. 1, lane 8). In singly transfected cells, upon immunoprecipitation of FLAG-β3 transfected cell extracts with anti-Myc antibodies or of Myc-β3 transfected cell extracts with anti-FLAG antibodies, no immunoreactive bands were detected on any immunoblots (Fig. 1, lanes 5 and 7).

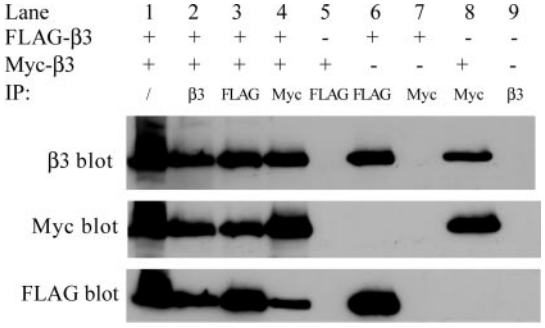

Fig. 1. Coimmunoprecipitation of differentially tagged full-length PLC-β3 constructs. Vectors encoding full-length human PLC-β3 fused to either amino-terminal FLAG tag (FLAG-β3; lanes 1–4, 6, and 7) or amino-terminal Myc tag (Myc-β3; lanes 1–5 and 8) were transfected into HEK 293 cells, either separately or together. Cells were harvested 48 h after transfection, and detergent cell extracts were immunoprecipitated with epitope-selective anti-FLAG antibody (lanes 3, 5, and 6), anti-Myc antibody (lanes 4, 7, and 8) or anti-PLC-β3 antibody (lanes 2 and 9). Immunoprecipitated sample from nontransfected HEK 293 detergent cell extract is shown in lane 9. Detergent cell extracts from Myc-β3 and FLAG-β3 cotransfected HEK 293 lysates precipitated by TCA are shown in lane 1. Precipitated samples were size separated by SDS-PAGE and immunoreactive proteins detected by immunoblot with anti-PLC-β3 antibody (top blot), anti-Myc antibody (middle blot), or anti-FLAG antibody (bottom blot). Shown are immunoreactive bands migrating at approximately 150 kDa by SDS-PAGE, representative of two independent experiments.

However, after cotransfection of both pCDNA3.1(+)-FLAG-PLC-β3 and pCMV-Myc-PLC-β3 into HEK 293 cells, either anti-Myc antibody (Fig. 1, lane 4) or anti-FLAG antibody (Fig. 1, lane 3) could immunoprecipitate protein bands of the expected molecular weight that were immunoreactive on blots developed with anti-Myc, anti-FLAG or anti-PLC-β3 antibodies (Fig. 1, lanes 3 and 4). These results demonstrate that coexpressed FLAG- and Myc-tagged PLC-β3s coprecipitate, probably as a result of formation of a PLC-β3 homodimer. Similar results were obtained when cells were extracted with a high-pH, detergent-free protocol rather than a detergent extraction protocol (data not shown), suggesting that detergent was not inducing oligomerization. Immunoprecipitation with anti-PLC-β3 antibodies of lysates from Myc-β3 and FLAG-β3 doubly transfected cells, followed by Western blot analysis of immunoprecipitates and densitometry, revealed that equivalent levels of each tagged construct were expressed in doubly transfected cells (Fig. 1, lane 2). Densitometric analysis of lanes 3 and 4 on the Myc and FLAG blots revealed that immunoprecipitation and immunodetection by opposite antibodies (e.g., IP:myc, FLAG blot) gave a signal 40 to 50% lower than immunoprecipitation and immunodetection by the same antibody. This reduction is expected in studies of homodimers, where three species are expected to form in any cotransfected cell (e.g., Myc-β3/Myc-β3, Myc-β3/FLAG-β3, and FLAG-β3/FLAG-β3) in a ratio of 1:2:1.

Identification of PLC-β1 Homodimers. To further investigate PLC-β isoenzyme dimerization, coimmunoprecipitation assays were performed with extracts of cells that had been transfected with vectors containing full-length PLC-β1 tagged at its amino terminus with either CFP or Myc epitopes (CFP-β1 or Myc-β1). The CFP-tagged PLC-β1 fragment was approximately 20 kDa larger than wild-type PLC-β1 by Western blot as expected (Fig. 2, lane 1). We found that differentially tagged full-length PLC-β1 constructs coimmunoprecipitated by either anti-GFP/CFP- or anti-Myc-selective antibodies are detectable on all immunoblots developed with anti-GFP/CFP-, anti-Myc-, or anti-PLC-β1-selective antibodies (Fig. 2, lanes 3 and 4), consistent with homodimer formation.

Attempts to Isolate PLC-β1 and PLC-β3 Heterodimers. To determine whether PLC-β1 and PLC-β3 were capable of forming heterodimers, immunoprecipitation assays were performed with extracts of endogenously expressing 1321N1 cells (Fig. 3A) and overexpressing HEK 293 cells transfected with pCDNA3.1(+)-FLAG-β3 and pCMV-Myc-β1 (Fig. 3B). PLC-β1 and PLC-β3 heterodimers were not detectable in either system. After 1321N1 cell lysis and extraction, immunoprecipitation with anti-PLC-β1 antibodies produced

immunoreactive bands only on immunoblots performed with anti-PLC-β1 and not anti-PLC-β3 antibodies. The converse immunoprecipitation experiments performed with anti-PLC-β3 antibodies yielded similar results (Fig. 3A). Similar results were observed after immunoprecipitation of extracts from HEK 293 cells cotransfected to express FLAG-β3 and Myc-β1. Immunoprecipitation with anti-Myc antibodies produced immunoreactive bands only on immunoblots performed with anti-PLC-β1 and not anti-PLC-β3 antibodies (Fig. 3B, lanes 2 and 6). Likewise, immunoprecipitation with anti-FLAG antibodies only produced immunoreactive bands on immunoblots performed with anti-PLC-β3 and not anti-PLC-β1 antibodies (Fig. 3B, lanes 1 and 4).

In addition, High-Five insect cells were coinfected with baculovirus constructs for the high-level coexpression of PLC-β1 and His_6PLC-β3. Ni-Sepharose chromatography of the cell lysate and immunoblot analysis of the column eluate showed that only His_6PLC-β3 adsorbed to the column (Fig. 3C, lanes 1–5). PLC-β1 was only found in the column flow-through (Fig. 3C, lanes 6 and 7), uncontaminated by full-length His_6PLC-β3. All data suggest that PLC-β1 and PLC-β3 do not form heterodimers, even when coexpressed in overexpressing cells.

PLC-β Monomer/Homodimer Equilibria Assessed by Size-Exclusion Chromatography. To further establish the oligomerization states of PLC-β homodimers, we used SEC to assess the potential for monomer–homodimer equilibria. PLC-β1, PLC-β2, and PLC-β3 have predicted molecular masses of 138.3, 133.7, and 138.8 kDa, respectively, as monomers, or 276.6, 267.4, and 277.6 kDa, respectively, as homodimers. Preparations of catalytically active PLC-β3 from exogenously expressing insect cells, loaded onto SEC at concentrations of 250 nM and greater, elute with an apparent molecular size of 330 kDa assessed compared with globular protein standards (Fig. 4, middle). These data are consistent with the idea that the enzyme exists as a relatively asymmetric dimer with a Stokes' radius of 5.3 nm under the indicated conditions.

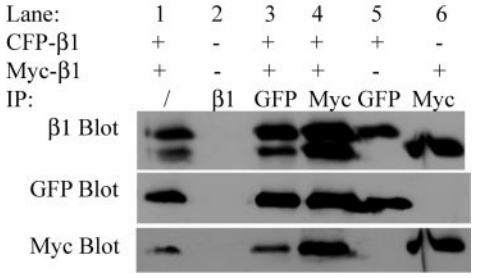

Fig. 2. Coimmunoprecipitation of differentially tagged full-length PLC-β1. Vectors with sequence encoding full-length PLC-β1 fused to either amino-terminal CFP tag (CFP-β1; lanes 1 and 3–5) or amino-terminal Myc tag (Myc-β1; lanes 1, 3, 4, and 6) were transfected into HEK 293 cells either separately or together. Cells were harvested 48 h after transfection, and detergent extracts were immunoprecipitated with anti-GFP/CFP antibody (lanes 3 and 5) or anti-Myc antibody (lanes 4 and 6). Detergent extracts from cell lysates of nontransfected HEK 293 were immunoprecipitated with anti-PLC-β1 antibodies (lane 2). Detergent extract from CFP-β1 and Myc-β1 cotransfected HEK 293 cell lysate was acid precipitated with TCA before immunoblotting (lane 1). Precipitated samples were size-separated by SDS-PAGE and immunodetected with anti-PLC-β1 antibody (top blot), anti-GFP/CFP antibody (middle blot), or anti-Myc antibody (bottom blot). Shown are immunoreactive bands migrating at approximately 150 kDa (β1 and Myc blots) and approximately 170 kDa (β1 and GFP blots) by SDS-PAGE, representative of two independent experiments.

Compared with overexpressed recombinant PLC-β3 from insect cells, native PLC-β3 (purified to >90% from endogenously expressing 1321N1 cells) eluted nearly identically at 305 kDa (data not shown). The purity of the preparation used in this experiment excludes the possibility that the high apparent molecular size results from a heterocomplex of PLC-β3 and some other protein.

PLC-β1 purified from baculovirus-infected insect cells also elutes as an apparent dimer of approximately 330 kDa (Fig. 4, top). Overnight incubation at 4°C of PLC-β1 or PLC-β3 resulted in a slight shifting of the elution peaks, suggesting that some minor dissociation of homodimer may result (Fig. 4, top and middle, dashed versus dotted smooth curves). At monomer loading concentrations $\leq$50 nM, Western blot-detected elution peaks of full-length PLC-β1 and PLC-β3 shift slightly and broaden a bit more toward the predicted elution volume of 13.1 ml for a monomer (Fig. 4, top and middle, squared traces). Reducing agents (DTT) did not affect the migration of PLC-β3 on the SEC column, suggesting that dimer formation is not dependent on disulfide bonds (data not shown).

PLC-β2 eluted as an apparent dimer at a loading concen-

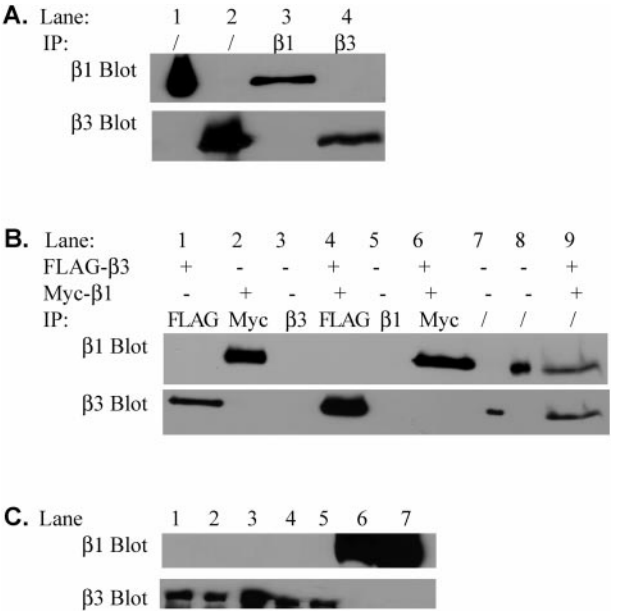

Fig. 3. No detection of heterodimer between PLC-β1 and PLC- β3. A, 1321N1 cells were lysed and detergent extracts were immunoprecipitated with anti-PLC-β1 antibody (lane 3) or anti-PLC-β3 antibody (lane 4) and were analyzed by immunoblot with anti-PLC-β1 antibody (top) or anti-PLC-β3 antibody (bottom). Purified PLC-β1 (0.5 μg; lane 1) and PLC-β3 (0.5 μg; lane 3) were included as controls. B, vectors containing sequence encoding either the full-length PLC-β3 fused to amino-terminal FLAG tag (FLAG-β3; lanes 1, 4, 6, and 9) or full-length PLC-β1 fused to amino-terminal Myc tag (Myc-β1; lanes 2, 4, 6, and 9) were transfected into HEK 293 cells either separately or together. Cells were harvested 48 h after transfection, and detergent extracts were immunoprecipitated with anti-FLAG antibody (lanes 1 and 4), anti-Myc antibody (lanes 2 and 6), anti-PLC-β3 antibody (lane 3), or anti-PLC-β1 antibody (lane 5). Detergent extract from FLAG-β3 and Myc-β1 cotransfected HEK 293 lysate was acid-precipitated with TCA (lane 9). Purified PLC-β1 (0.5 μg; lane 8) and PLC-β3 (0.5 μg; lane 7) were included as controls. Samples were size separated by SDS-PAGE and immunodetected by antibodies to PLC-β1 (top) or PLC-β3 (bottom). C, after purification, using nickel affinity resin, of lysates from High-Five insect cells coinfected to overexpress both His_6-tagged PLC-β3 and PLC-β1, column fractions (1–7) were analyzed by immunoblot with anti-PLC-β1 antibody (top) or anti-PLC-β3 antibody (bottom). Lanes 1 to 5 represent fractions eluted with 250 mM imidazole; lanes 6 and 7 represent the column flow-through.

tration of 2.8 μM, corresponding to a molecular mass of 330 kDa, compared with the predicted monomeric molecular mass of 133.7 kDa (Fig. 4, bottom, solid smooth curve). However, in contrast to PLC-β1 or PLC-β3, the elution profile of PLC-β2 at 200 nM became increasingly biphasic with incubation time (Fig. 4, bottom, dashed versus dotted smooth curves). Peak concentrations after 4°C overnight incubation of PLC-β2 at 200 nM corresponded to apparent molecular sizes of 240 and 120 kDa, suggesting that PLC-β2 homodimer dissociates at <200 nM because of a lower homodimeric affinity than PLC-β1 or PLC-β3. SDS-PAGE analysis of the fractionated elute confirmed that the biphasic elution profile of PLC-β2 was not the result of degradation (data not shown).

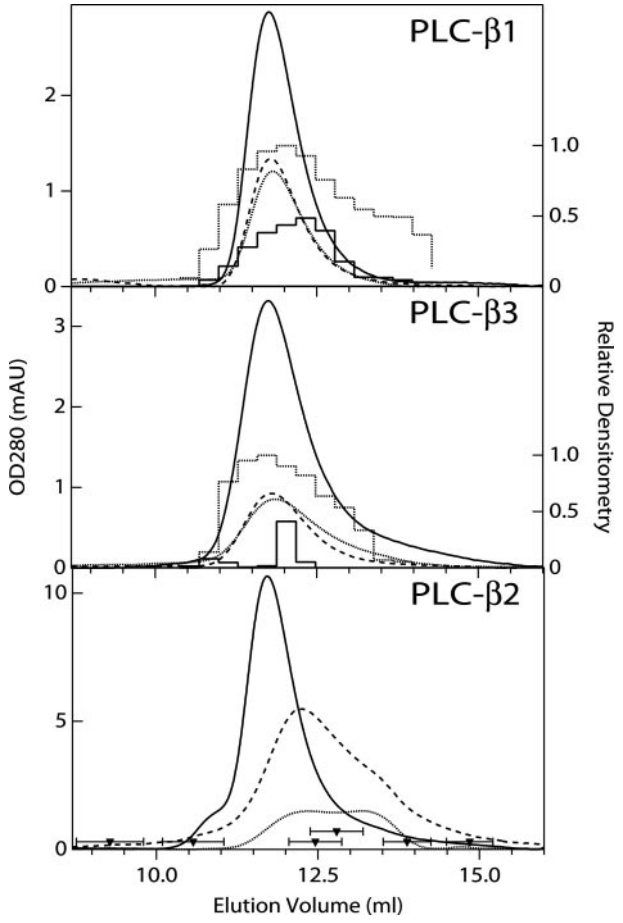

Fig. 4. Analytical size-exclusion chromatography of PLC-β1, PLC-β2, and PLC-β3 isolated from High-Five cells. A Superdex 200 column (Vo = 8.04 ml, Vi = 20.46 ml) was operated as described under *Materials and Methods* and calibrated with thyroglobulin (669 kDa), ferritin (232 kDa), catalase (232 kDa), aldolase (158 kDa), bovine serum albumin (67 kDa), and ovalbumin (43 kDa). Calibration standard peak positions (Ve) are indicated at the bottom of the figure (▼); associated error bars indicate trace widths at half-height of standards. Elution profiles for experimental samples loaded at concentrations of 250 nM and greater were recorded as absorbance at 280 nm (smooth curves). Elution profiles of 50 nM and less concentrated samples, collected in 0.3 ml aliquots, were analyzed by Western blot and quantitated by Densitometry (squared line histogram traces). Varying concentrations of size-exclusion purified samples of PLC-β were maintained on ice for the indicated times in parentheses. PLC-β1 (top): 482 nM (31 h, solid curve) eluted at 11.76 ml; 250 nM (3 h, dashed curve) eluted at 11.79 ml; 250 nM (24 h, dotted curve) eluted at 11.84 ml; 50 nM (22 h) elution peak was centered at 12.0 ml (dotted squared line); and 10 nM (5 h) was centered at 12.3 ml (solid squared line). PLC-β3 (middle): 717 nM (29 h, solid curve) eluted at 11.75 ml; 250 nM (1.5 h, dashed curve) at 11.81 ml; 250 nM (27 h, dotted curve) at 11.87 ml; 50 nM (20 h) elution peak was centered at 11.7 ml (dotted squared line); and 10 nM (8 h) was centered at 12.0 ml (solid squared line). PLC-β2 (bottom): 2.8 μM (0 h, solid curve) eluted as single peak at 11.71 ml; 200 nM (2 h, dashed curve) eluted at 12.22 ml with a shoulder at approximately 13.5 ml; 200 nM (18 h, dotted curve) resolved into two peaks centered at 12.28 and 13.23 ml.

Mapping of the Domains Involved in PLC-β3 Dimerization. To further delineate the domains involved in dimerization of PLC-β3, and to identify the location of the dimerization domains, four different truncated fragments of PLC-β3, tagged with either FLAG, Myc, or CFP epitopes, were constructed (Fig. 5A). These fragments included the amino-terminal PH/EF hand domains (NT-β3), the C-tail domain (CT-β3), the catalytic X and Y domains (XY-β3), and C2/C-tail-deleted PLC-β3 (ΔC-β3). In whole-cell assays of transfected HEK 293 cells, the catalytic Myc-XY-β3 fragment increased inositol phospholipid hydrolysis 2-fold, similar to the basal (non–G-protein-stimulated) activity of transfected full-length PLC-β3. After cotransfection into HEK 293 cells, FLAG and Myc epitope-tagged ΔC-β3 (Fig. 5B), CFP and Myc epitope-tagged XY-β3 (Fig. 5C), and CFP and Myc epitope-tagged CT-β3 (Fig. 5D) can be immunoprecipitated from cell extracts by an anti-epitope antibody and detected on immunoblot with either the same or the opposite anti-epitope antibody. For example, immunoprecipitation of FLAG- and Myc-tagged ΔC-β3 with anti-FLAG antibodies results in immunoreactivity on blots incubated with either anti-FLAG or anti-Myc antibodies at the predicted molecular weight (Fig. 5B, lanes 4 and 5). As expected, CFP-tagged fragments were detectable on immunoblot migrating approximately 20 kDa larger than Myc- or FLAG-tagged constructs (Fig. 5, C and D). These results suggested that fragments containing the C-tail and/or catalytic X and Y domains form dimers independent of full-length protein. However, the differentially tagged fragments containing C-tail or catalytic domains were not equally detectable to full-length protein on immunoblots after coimmunoprecipitation with the opposite antibody, suggesting that the subdomains may have lower affinities as homodimers than as full-length PLC-β3. For example, densitometric analysis of Western blots demonstrated that immunoprecipitation of FLAG-ΔC-β3/Myc-ΔC-β3 with anti-FLAG antibodies reproducibly results in less than 20% of the signal on anti-Myc blots compared with anti-FLAG blots (Fig. 5B, lanes 4 and 5). The same principle is observed with XY-β3 and CT-β3 (Fig. 5C, lanes 3 versus 4; Fig. 5D, lanes 2 versus 3).

FLAG-NT-β3 and Myc-NT-β3, fragments of PLC-β3 devoid of catalytic and carboxyl-terminal domains, did not seem to dimerize. FLAG-NT-β3 and Myc-NT-β3, containing the PH and EF hand domains of PLC-β3, produced only immunoreactive bands when immunoprecipitated from transfected HEK cell extracts and detected by immunoblot with the same anti-epitope antibody. FLAG-NT-β3 is not immunoprecipitated by anti-Myc epitope antibody, and Myc-NT-β3 is not immunoprecipitated by anti-FLAG epitope antibody (Fig. 5E). Thus, the PH and EF hand domains fragment of PLC-β3 seemed to exist as a monomer when independent of full-length protein.

FRET Analysis of PLC-β Homodimer and Heterodimer Status in Whole Cells. The oligomerization status of PLC-β3 was assessed in whole cells by microscopic FRET. HEK 293 cells were transfected with pECFP-C2-PLC-β3 (CFP-PLC-β3), pEYFP-N2-PLC-β3 (PLC-β3-YFP), or pCDNA3.1(+)-YFP-PLC-β3 (YFP-PLC-β3). All three

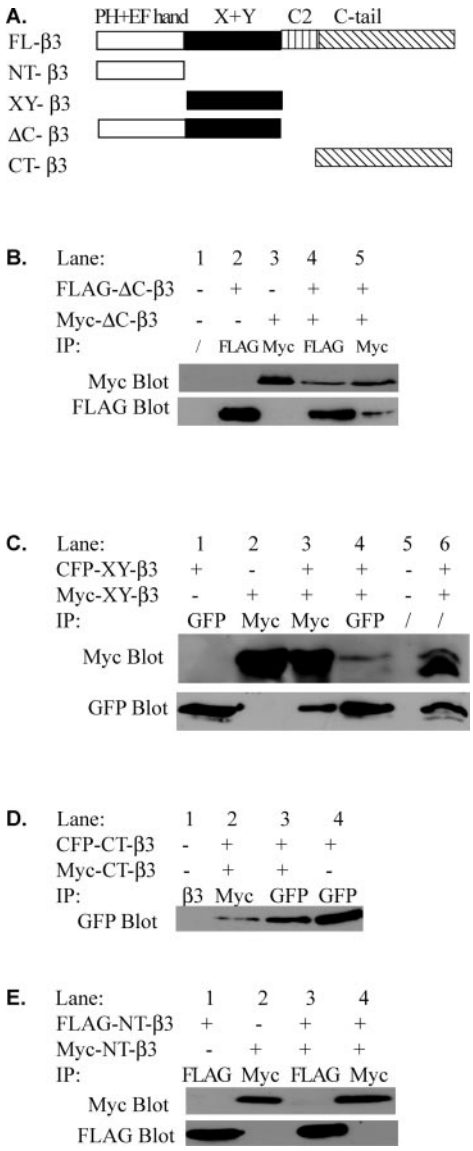

Fig. 5. Coimmunoprecipitation of differentially tagged PLC-β3 subdomain fragments. A, shown is a linear schematic of PLC-β3 fragments according to putative structural subdomains based on sequence similarity to known protein structural motifs. White bar indicates fragments spanning a putative PH domain and four EF hand domains (PH + EF hand). The black bar indicates a fragment spanning the catalytic X and Y domains and intervening domain (X + Y). The vertically hatched bar indicates a fragment with similarity to C2 domains (C2), and the diagonally hatched bar represents a fragment encompassing the structurally unique carboxyl-terminal third of the protein (C tail). B, vectors containing sequence for PLC-β3 C2/C-tail deletion mutants fused to either amino-terminal FLAG tag (FLAG-ΔCβ3; lanes 2, 4, and 5) or amino-terminal Myc tag (Myc-ΔCβ3; lanes 3, 4, and 5) were transfected into HEK 293 cells either separately or together. Cells were harvested 48 h after transfection and detergent extracts were immunoprecipitated with epitope-selective anti-FLAG antibody (lanes 2 and 4) or anti-Myc antibody (lanes 3 and 5). Detergent extracts from nontransfected HEK 293 cells were also precipitated by TCA (lane 1). Precipitated samples were size separated by SDS-PAGE and immunoreactive proteins detected with anti-Myc antibody (top blot) or anti-FLAG antibody (bottom blot). Shown are immunoreactive bands migrating at approximately 80 kDa by SDS-PAGE, representative of two independent experiments. C, vectors containing sequence encoding the catalytic domain of PLC-β3 fused to either amino-terminal CFP tag (CFP-XY-β3; lanes 1, 3, 4, and 6) or amino-terminal Myc tag (Myc-XY-β3; lanes 2–4 and 6) were transfected into HEK 293 cells either separately or in combination. Detergent extracts of transfected cell were immunoprecipitated with anti-GFP/CFP antibody (IP: GFP, lanes 1 and 4) or anti-Myc antibody (IP:Myc, lanes 2 and 3). Detergent cell extracts from nontransfected HEK 293 cell lysate (IP:/, lane 5) or cotransfected HEK 293 cell lysate (IP:/, lane 6) were precipitated by TCA as controls. Precipitated samples were immunodetected with anti-Myc antibody (top blot) or anti-GFP/CFP antibody (bottom blot). Shown are immunoreactive bands migrating at approximately 50 kDa (top blot) and approximately 70 kDa (bottom blot) by SDS-PAGE, representative of two independent experiments. D, vectors containing sequence encoding the C-tail domain of PLC-β3 fused to either amino-terminal CFP tag (CFP-CT-β3; lanes 2–4) or amino-terminal Myc tag (Myc-CT-β3; lanes 2 and 3) were transfected into HEK 293 cells either separately or together. Detergent cell extracts were immunoprecipitated with anti-β3 antibody (lane 1), anti-GFP antibody (lanes 3 and 4), or anti-Myc antibody (lane 2), and immunodetected with anti-GFP/CFP antibody. Shown are immunoreactive bands migrating at approximately 80 kDa by SDS-PAGE, representative of two independent experiments. E, Vectors containing sequence encoding the amino-terminal PH and EF hand domains of PLC-β3 fused to either amino-terminal FLAG tag (FLAG-NT-β3; lanes 1, 3, and 4) or amino-terminal Myc tag (Myc-NT-β3; lanes 2–4) were transfected into HEK 293 cells either separately or together. Detergent cell extracts were immunoprecipitated with anti-FLAG antibody (lanes 1 and 3) or anti-Myc antibody (lanes 2 and 4) and immunoreactive proteins detected with anti-Myc antibody (top blot) or anti-FLAG antibody (bottom blot). Shown are immunoreactive bands migrating at approximately 40 kDa by SDS-PAGE, representative of two independent experiments.

PLC-β3 plasmids expressed at similar levels in HEK 293 cells as assessed by Western blot (data not shown).

Transfected HEK 293 cells were examined for YFP and CFP emission at >530 nm and 470 to 500 nm, respectively, using a confocal fluorescent microscope. Overlap between the channels was undetectable as assessed by expressing YFP- and CFP-tagged constructs independently (Karpova et al., 2003). Shown is a representative image of a CFP-PLC-β3/PLC-β3-YFP doubly transfected cell in the YFP emission channel (Fig. 6, right) and CFP emission channel (Fig. 6, left). A selected cell region was photobleached in the YFP channel, and prebleach (Fig. 6, top) and postbleach images (Fig. 6, bottom) were collected. The postbleach images display an almost complete loss of YFP intensity as a result of YFP photobleaching and a concurrent gain in CFP intensity in the bleached regions, indicative of fluorophore coupling.

FRET efficiencies based on donor intensity increases after acceptor photobleaching were calculated as described under *Materials and Methods*. The average FRET efficiency for cells transfected with both CFP-PLC-β3 and PLC-β3-YFP, which express CFP and YFP at opposite termini of PLC-β3, was 5.7 $\pm$ 0.4% (n = 52), statistically different compared with

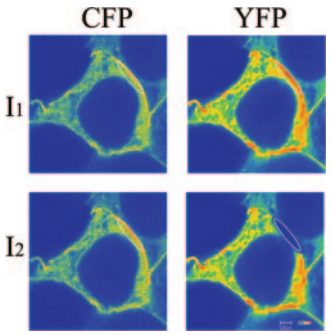

Fig. 6. FRET in HEK 293 cells cotransfected with CFP-β3 and β3-YFP plasmids. HEK 293 cells were cotransfected with vectors constructed to express full-length PLC-β3 fused with CFP or YFP at the amino or carboxyl terminus, respectively. Pseudocolored cell images obtained in the YFP emission channel using a LP540 nm filter (YFP, top) and in the CFP emission channel using a 470–500 nm filter (CFP, bottom) are shown immediately before (I_1) and after (I_2) photobleaching as described under *Materials and Methods*. The region isolated for photobleaching is indicated by the outlined oval. Scale bar, 2 μm. This image represents 52 similarly analyzed images.

cells cotransfected with CFP- and YFP-containing control plasmids, or with CFP-PLC-β3 alone (Table 1). In contrast, FRET experiments using a different PLC-β3 FRET pair, CFP-PLC-β3 and YFP-PLC-β3, both of which express CFP and YFP at the amino terminus of PLC-β3, gave an average FRET efficiency of 3.0 ± 0.6%, which was not different from controls but was different from the PLC-β3 FRET pair tagged at opposite ends (Table 1).

We obtained no evidence of PLC-β1/PLC-β3 heterodimers in cotranfected cells by FRET analysis. FRET efficiency for cotransfected CFP-PLC-β1 and PLC-β3-YFP (fluorescent tags at opposite ends) cells or for cotransfected CFP-PLC-β1 and YFP-PLC-β3 (fluorescent tags at amino termini) was no different from control CFP/YFP cotransfected cells (Table 1).

The FRET efficiency for coupling between CFP-PLC-β3 and PLC-β3-YFP in doubly transfected cells was not dependent on expression levels of the proteins. To control for protein expression effects on FRET efficiency, differing total amounts of CFP-PLC-β3 and PLC-β3-YFP plasmids were cotransfected into HEK 293 cells at a constant plasmid ratio of 1:1. As expected, FRET analysis of cells transfected with CFP-PLC-β3 and PLC-β3-YFP at three different total DNA concentrations (0.05, 0.1, and 0.9 μg) revealed that FRET efficiencies did not vary significantly (6.2 ± 0.5, 6.3 ± 0.4, and 5.4 ± 0.8%, respectively; n = 20–23) with varying DNA concentrations. However, overall fluorescence intensity did increase as expected for increased protein expression with increasing DNA transfected.

Using the average FRET efficiency value of 5.7% from the CFP-PLC-β3 and PLC-β3-YFP doubly transfected cells and a Förster distance for CFP/YFP pairs of 4.9 nm as calculated previously (Patterson et al., 2000; Karpova et al., 2003), we calculated the distance between the two fluorophores linked to opposite ends of full-length PLC-β3 to be 7.8 nm.

Discussion

Using coimmunoprecipitation, SEC, and microscopic FRET analyses, we have demonstrated for the first time that full-length PLC-β isoenzymes can form homodimers in whole cells and crude cell extracts, suggesting that previous detection of PLC-β homodimers was not an artifact of purification or concentration (Singer et al., 2002).

Based on our data with various fragments of PLC-β3, we conclude that at least two subdomains of PLC-β3 are involved in dimer formation: one in the catalytic X and Y domains, and the other in the carboxyl-terminal C-tail domain. The extensive contacts between the C-tail dimers of turkey PLC-β in the crystal structure of Singer et al. (2002) suggest that the C-tail domain should be sufficient to maintain dimerization of the full-length protein. Although this is not disputed, additional sequence in the catalytic domain of PLC-β3 will dimerize independent of the C-tail. PLC-δ1, which lacks the C-tail motif of PLC-β isoenzymes, also purifies as a dimer (Ellis et al., 1993), reinforcing the idea that the catalytic domains may participate in the dimer association. Based on our coprecipitation studies, the C-tail and catalytic domain fragments of PLC-β3 seem to self-associate with somewhat less affinity than the full-length protein, suggesting that both domains play a role in high-affinity homodimerization.

Using whole cell fluorescence microscopy, we observed fluorophore coupling between CFP and YFP when placed at opposite ends of full-length PLC-β3 for coexpression. The FRET efficiency between CFP-PLC-β3 and YFP-PLC-β3, in which CFP and YFP were placed at the same amino terminal end of full-length PLC-β3, was significantly lower than the oppositely placed fluorophore PLC-β3 FRET efficiency (p < 0.001). The FRET data obtained with oppositely and similarly oriented CFP and YFP constructs suggest that opposite termini in PLC-β3 may be in closer proximity than the same termini in the dimer structure. This result is consistent with the antiparallel orientation of the homodimerized turkey PLC-β carboxyl-terminal fragments upon crystallization. The crystallized turkey PLC-β C tail formed a structure of three long α-helices, labeled A, B, and C, of which part of αA and most of αB were involved in more extensive dimeric contacts along the long length of the dimer. Singer et al. (2002) noted that the most highly conserved amino acids among the C tails of PLC-β isoenzymes were not in the dimer contact regions but in the $G\alpha_q$-regulated regions, suggesting that amino acids in the αB helix may play a role in the homodimeric specificity of PLC-β1 and PLC-β3.

The average FRET efficiency that we observed for oppositely oriented CFP- and YFP-tagged PLC-β3, 5.7%, is small but not without precedent in the literature for homodimers. Homodimerization of unstimulated leptin b receptors yields FRET efficiencies of 4.9% by the acceptor photobleaching method, the same method used in this study (Biener et al., 2005). Homodimers are expected to yield FRET signals that are half the intensity of heterodimers, resulting from the unavoidable formation of YFP-β3/YFP-β3 dimer and CFP-β3/CFP-β3 dimers that do not yield FRET signals upon acceptor photobleaching. In addition, our data demonstrating that acceptor photobleaching FRET efficiency between CFP-β3 and β3-YFP does not vary with varying DNA concentrations provides evidence that the FRET signal is not an artifact based on increasing fluorescence intensity with increasing expression levels.

FRET efficiency was used to calculate a distance of approximately 8 nm between CFP and YFP tags linked to opposite ends of PLC-β3. SEC data estimates an intramolecular diameter of 11 nm for PLC-β3. At a distance of 8 nm, the CFP and YFP tags are calculated to be within the hydrodynamic diameter of a dimeric PLC-β3. However, the calculation of distance between fluorescence resonance pairs, based on the Förster distance of isolated CFP and YFP, is complicated by many factors, including the flexibility of linkers and the mobility of the CFP and YFP tags.

PLC-β1 and PLC-β3 are often coexpressed, and because they exist separately as homodimers, the possible formation of heterodimers was tested by attempting to coimmunopre-

TABLE 1

FRET efficiency between various PLC-β3 and PLC-β1 fluorescently tagged pairs in transfected HEK 293 cells

FRET efficiency was assessed by the acceptor photobleaching protocol in HEK 293 cells transfected to express the indicated constructs. Data represent the mean ± S.E. for the number of cells indicated (n).

Transfection	FRET Efficiency
CFP-PLC-β3 + PLC-β3-YFP	5.7 ± 0.4% (n = 52)
CFP-PLC-β3	−0.6 ± 0.7% (n = 32)***
CFP + YFP	3.0 ± 0.4% (n = 30)***
CFP-PLC-β3 + YFP-PLC-β3	3.0 ± 0.6% (n = 29)***
CFP-PLC-β1 + PLC-β3-YFP	2.1 ± 0.5% (n = 31)***
CFP-PLC-β1 + YFP-PLC-β3	3.2 ± 0.7% (n = 21)**

** P < 0.01 or *** P < 0.001, a statistically significant FRET efficiency difference between CFP-PLC-β3 + PLC-β3-YFP transfected cells and all other controls.

cipitate both isoenzymes from natively expressing 1321N1 cells; from cotransfected, overexpressing HEK 293 cells; by attempting copurification from overexpressing baculovirus-infected insect cells; or by microscopic FRET analysis of PLC-β3-YFP and CFP-PLC-β1 cotransfected cells. We found that PLC-β3 does not form a heterodimer with PLC-β1 within detection limits under conditions in which homodimers are easily detected.

Full-length PLC-β3 seems to form a high-affinity, catalytically active homodimer that is not dependent on disulfide bonds and is resistant to detergent dissociation with 0.5% octyl-β-D-glucopyranoside, 500 mM NaCl, or pH 10 extraction. Analytical SEC data suggest that PLC-β1 and PLC-β3 are predominantly homodimeric at monomer concentrations in excess of 0.2 μM. Broadening and slight rightward shifting toward lower molecular size of SEC peaks below 0.2 μM for PLC-β1 and PLC-β3 suggest that a small amount of monomer/homodimer interconversion occurs at physiological concentrations (estimated as approximately 10 nM or less in 1321N1 cell cytosol). For comparative purposes, we obtained experimental data on PLC-β2 oligomeric status. Guo et al. (2005) reported that purified PLC-β2 migrated as a monomer. Under our purification conditions, PLC-β2, like PLC-β1 and PLC-β3, seems to form homodimers. Although protein detection limits restrict quantitation of the homodimer dissociation constants, the dimeric dissociation constant for PLC-β2 is clearly greater than the same constant for PLC-β1 or PLC-β3. Thus, the physiologic monomer/homodimer distribution of PLC-β2 is probably dependent on intracellular concentrations, whereas PLC-β3 is predicted to exist nearly exclusively as a homodimer. The lower affinity of PLC-β2 homodimers may allow for alternative heterodimer formations with PLC-δ partners, as suggested previously (Guo et al., 2005). Considering that PLC-δ lacks a C tail domain, perhaps PLC-β2/PLCδ association occurs through the catalytic domains, consistent with our data demonstrating association of PLC-β3 catalytic fragments.

Cooperative protein dimers commonly decrease the range of activator concentrations over which an enzyme converts from fully inactive to fully active. PLC-β isoenzymes display steep concentration-dependence curves for G protein activation, supporting a cooperative homodimer model (Boyer et al., 1992; Paterson et al., 1995; Paulssen et al., 1996). In addition, by studying PLC-β1 C-tail fragments or deletion mutants, Paulsen et al. (1996) and Ilkaeva et al. (2002) suggested that the GTPase activating protein activity and $G\alpha_q$ activation of PLC-β1 may depend on the dimerization of the C-tail domain.

The existence of homo- and heterodimers of G protein-coupled receptors has gained widespread acceptance (Milligan, 2004). Heteroligomeric G protein-coupled receptor signaling complexes might easily incorporate PLC-β effector pairs. Indeed, the crystal structure of PLC-βT C tail dimer was modeled to accommodate docking of two molecules of $G\alpha_q$ (Singer et al., 2002). A full understanding of the physiologic role of PLC-β dimerization will require accurate modeling of these enzymes' native microenvironments, including the subplasmalemmal surface and interactions with a wide array of potential binding partners.

Acknowledgments

We gratefully acknowledge the microscopy assistance provided by Thuan Tran and Tamara Fraley of the Confocal Microscopy Facility at Oregon State University. We thank Dr. Mark Leid and Acharawan Khamasiritrakul (College of Pharmacy, Oregon State University) for providing transfectable HEK 293 cells, helpful discussions, and assistance with techniques. We are grateful to Kristi Crofoot for continuing laboratory support and George Estreich for editing of the manuscript.

References

Avram D, Ishmael JE, Nevrivy DJ, Peterson VJ, Lee SH, Dowell P, and Leid M (1999) Heterodimeric interactions between chicken ovalbumin upstream promoter-transcription factor family members ARP1 and ear2. *J Biol Chem* **274:**14331–14336.

Biener E, Charlier M, Ramanujan KV, Daniel N, Eisenberg A, Bjorbaek C, Herman B, Gertler A, and Djiane J (2005) Quantitative FRET imaging of leptin receptor oligomerization kinetics in single cells. *Biol Cell* **97:**905–919.

Boyer JL, Waldo GL, and Harden TK (1992) βγ-Subunit activation of G-protein-regulated phospholipase C. *J Biol Chem* **267:**25451–25456.

Chubet RG and Brizzard BL (1996) Vectors for expression and secretion of FLAG epitope-tagged proteins in mammalian cells. *Biotechniques* **20:**136–141.

Ellis MV, Carne A, and Katan M (1993) Structural requirements of phosphatidylinositol-specific phospholipase Cδ1 for enzyme activity. *Eur J Biochem* **213:**339–347.

Filtz TM, Li Q, Boyer JL, Nicholas RA, and Harden TK (1994) Expression of a cloned P_2Y-purinergic receptor that couples to phospholipase C. *Mol Pharmacol* **46:**8–14.

Filtz TM and Niibori Y (2004) Desensitization of angiotensin-stimulated inositol phosphate accumulation in human vascular smooth muscle cells. *Eur J Pharmacol* **502:**11–19.

Fukami K (2002) Structure, regulation, and function of phospholipase C isozymes. *J Biochem (Tokyo)* **131:**293–299.

Guo Y, Rebecchi M, and Scarlata S (2005) Phospholipase Cβ2 binds to and inhibits phospholipase Cδ1. *J Biol Chem* **280:**1438–1447.

Hansen CA, Schroering AG, and Robishaw JD (1995) Subunit expression of signal transducing G proteins in cardiac tissue: implications for phospholipase C-β regulation. *J Mol Cell Cardiol* **27:**471–484.

Ilkaeva O, Kinch LN, Paulssen RH, and Ross EM (2002) Mutations in the carboxyl-terminal domain of phospholipase C-β1 delineate the dimer interface and a potential $G\alpha_q$ interaction site. *J Biol Chem* **277:**4294–4300.

Kapust RB, Tözser J, Fox JD, Anderson DE, Cherry S, Copeland TD, and Waugh DS (2001) Tobacco etch virus protease: mechanism of autolysis and rational design of stable mutants with wild-type catalytic proficiency. *Protein Eng* **14:**993–1000.

Karpova TS, Baumann CT, He L, Wu X, Grammer A, Lipsky P, Hager GL, and McNally JG (2003) Fluorescence resonance energy transfer from cyan to yellow fluorescent protein detected by acceptor photobleaching using confocal microscopy and a single laser. *J Microsc* **209:**56–70.

McCullar JS, Larsen SA, Millimaki RA, and Filtz TM (2003) Calmodulin is a phospholipase C-β interacting protein. *J Biol Chem* **278:**33708–33713.

Milligan G (2004) G protein-coupled receptor dimerization: function and ligand pharmacology. *Mol Pharmacol* **66:**1–7.

Paterson A, Boyer JL, Watts VJ, Morris AJ, Price EM, and Harden TK (1995) Concentration of enzyme-dependent activation of PLC-β1 and PLC-β2 by $G\alpha_{11}$ and βg subunits. *Cell Signaling* **7:**709–720.

Paterson A, Filtz TM, and Harden TK (1997) Baculovirus-promoted expression, purification, and functional assay of G-protein regulated PLC-β isoenzymes, in *Signaling by Inositol Lipids and Inositol Phosphates* (Shears S ed) pp 85–98, Oxford University Press.

Patterson GH, Piston DW, and Barisas BG (2000) Forster distances between green fluorescent protein pairs. *Anal Biochem* **284:**438–440.

Paulssen RH, Woodson J, Liu Z, and Ross EM (1996) Carboxyl-terminal fragments of phospholipase C-beta1 with intrinsic Gq GTPase-activating protein (GAP) activity. *J Biol Chem* **271:**26622–26629.

Rhee S-G (2001) Regulation of phosphoinositide-specific phospholipase C. *Annu Rev Biochem* **70:**281–312.

Saunders CM, Larman MG, Parrington J, Cox LJ, Royse J, Blayney LM, Swann K, and Lai FA (2002) PLC zeta: a sperm-specific trigger of Ca^{2+} oscillations in eggs and embryo development. *Development* **129:**3533–3544.

Siegel LM and Monty KJ (1966) Determination of molecular weights and frictional ratios of proteins in impure systems by use of gel filtration and density gradient centrifugation. Application to crude preparations of sulfite and hydroxylamine reductases. *Biochim Biophys Acta* **112:**346–362.

Singer AU, Waldo GL, Harden TK, and Sondek J (2002) A unique fold of phospholipase C-β mediates dimerization and interaction with Gαq. *Nat Struct Biol* **9:**32–36.

Snyder JT, Singer AU, Wing MR, Harden TK, and Sondek J (2003) The pleckstrin homology domain of phospholipase C-β2 as an effector site for Rac. *J Biol Chem* **278:**21099–21104.

Address correspondence to: Theresa M. Filtz, 203 Pharmacy Building, Oregon State University, Corvallis, OR 97331-3507. E-mail: theresa.filtz@oregonstate.edu